Journal of Industrial and Management Optimization

https://www.aimspress.com/journal/jimo

JIMO, 22(3): 1394–1418.
DOI:10.3934/jimo.2026051
Received: 23 September 2025
Revised: 09 January 2026
Accepted: 22 January 2026
Published: 12 February 2026

Research article

A distributionally robust optimization framework for attribute-independent preference estimation

Lingyun Ji and Dali Zhang*

Antai College of Economic and Management, Shanghai Jiao Tong University, 200030, Shanghai, China

* **Correspondence:** Email: zhangdl@sjtu.edu.cn.

Abstract: In this paper, we introduced a framework that requires only choice data to learn a decision-maker's utility, unlike the classic random utility framework which needs historical choices and multiple attributes. We proposed a two-stage optimization model for the single decision-maker's discrete choice processes with sequential uncertainties. In the first stage, the decision-maker made a strategic choice that stochastically determined the set of future alternatives. In the second stage, after these alternatives were realized, the decision-maker made a final operational choice to maximize utility. The second stage was modeled as a distributionally robust optimization problem with a Kullback–Leibler divergence constraint, enabling worst-case utility evaluation. This model built an ambiguity set from historical choice data to define possible distributions for the decision-maker's preferences. We also analyzed the problem's convexity and used an augmented Lagrangian algorithm to find the optimal solution. Extensive numerical experiments, including case studies and in-depth sensitivity analyses, demonstrated the method's effectiveness.

Keywords: utility preference; distributionally robust optimization; Kullback-Leibler divergence
Mathematics Subject Classification: 90C15, 90C47, 90B50, 90B06

1. Introduction

The random utility model (RUM) is widely used for modeling choice behavior, wherein a decision-maker aims to maximize utility by selecting an alternative from a choice set. The foundational research on RUM dates back to Thurstone [1], with its modern economic formulation being formally developed by Marschak [2]. In recent years, the RUMs have been integrated into decision-making studies across application areas, including investment, marketing, policy-making, and product design [3–6]. Despite its widespread application, two significant challenges persist in learning the decision-maker's utility. The first is the assumption of the availability of the utility function structures and the attribute data of alternatives [7]. The second challenge arises from the decision-maker's uncertainty regarding their future preferences for different alternatives. These challenges become more critical in sequential settings, where an early strategic decision such as supplier selection or research and development investment planning probabilistically shapes the set of operational choices available later. In such settings, missing attribute data and uncertainty in future preferences may lead to suboptimal decisions with long-term consequences. To address these challenges, we develop a sequential decision framework that identifies the optimal commitment strategy while explicitly accounting for missing attribute data and uncertain future preferences.

In this study, we formalize this challenge as a two-stage sequential planning problem for a single decision-maker. In the first stage, the decision-maker selects a strategy m from a set of candidate strategies $\{1, \ldots, M\}$. This choice determines the probabilistic availability of the alternatives $\mathcal{K} = \{0, \ldots, K\}$ in the subsequent stage. Specifically, selecting strategy m defines a vector $\theta^m = (\theta_0^m, \ldots, \theta_K^m)^\top \in [0, 1]^{K+1}$, where θ_k^m represents the probability that alternative k will be available to the decision-maker in the second stage. In the second stage, facing the randomly realized set of available alternatives and their associated random utilities (influenced by the underlying true preferences), the decision-maker makes a choice to maximize their realized utility. Our overall goal is to find the optimal first-stage strategy m by solving a distributionally robust optimization (DRO) problem that considers the worst-case expected utility over the ambiguity set of preferences. The first-stage decision in our problem relates to the concept of *consideration sets* [8, 9], but with the key difference that the availability of alternatives within the set resulting from the first-stage choice is probabilistic ($\theta_k^m \in [0, 1]$) rather than deterministic. Our approach also differs from randomized assortment optimization [10], where randomization occurs only at the assortment level and does not influence the decision making problem in the second stage.

Our work relates to several research areas. The sequential characteristic of our problem, where the decision-maker faces ambiguity about their own future preferences [11, 12], gives rise to a strategic formulation. The first-stage decision can be interpreted as a form of precommitment in the sense of behavioral economics, where an agent restricts their future choice set to mitigate self-control problems or uncertainty about future preferences [13]. From a modeling perspective, our framework contributes to the growing literature on preference robust optimization (PRO). The PRO literature has significantly advanced decision-making with incomplete utility information by constructing ambiguity sets over utility functions [14–17]. Our work is particularly related to developments in multistage PRO [18], which address dynamic decision-making under preference ambiguity. However, a key distinction of our work is its focus on discrete choice outcomes in an attribute-independent setting, which remains underexplored.

From a technical perspective, our approach tackles two fundamental challenges in choice modeling. The first is the reliance of classical RUM on observed attributes of alternatives [19]. Obtaining complete and accurate attribute data are often impractical, leading to biased estimations [20–22]. While methods such as Bayesian imputation [23] and inverse modeling [24] have been proposed to mitigate this issue, our framework formalizes an attribute-independent utility measure based solely on choice probabilities without the need for attribute data. The second challenge stems from the inherent uncertainty in these choice probabilities. To address this, researchers have applied DRO to choice modeling and assortment problems [25–27]. However, DRO frameworks are typically built upon attribute-based utility structures. To the best of our knowledge, the integration of a DRO approach with an attribute-independent preference model remains an open gap in the literature. Thus, we aim to fill this gap by proposing a framework that handles preference ambiguity in a setting where attribute data are not required.

The main contribution of this study is two-fold. First, we evaluate strategies m in the first stage without imposing any assumptions on the specific functional form of their utility. Second, we account for uncertainty in decision-maker preferences by applying a DRO approach to identify the worst-case scenario for the decision-maker's utility. As a result, our model requires only decision-makers' historical choice data to compute the expected utility for a given strategy m under uncertainties in preferences and future availability.

The remainder of the paper is organized as follows: In Section 2, we present a two-stage model and define the ambiguity set of uncertainties. In Section 3, we investigate the conditions under which the problem is convex and present the corresponding optimality conditions. In addition, an augmented Lagrangian algorithm is employed to solve this problem. Finally, in Section 4, we present numerical experiments to demonstrate the effectiveness of the method.

2. Model

Before presenting the model, we summarize the notation used throughout the paper in Table 1.

Table 1. Notation summary.

Symbol	Description
$\mathcal{K}$	The set of alternatives, $\{0, 1, \ldots, K\}$.
$\mathscr{K}$	The set of all non-empty subsets of $\mathcal{K}$.
k	The index of alternative.
m	The first-stage strategy chosen by the decision-maker.
θ_k^m	The probability that alternative k is available under strategy m.
$\mathcal{K}_m$	The randomly realized set of available alternatives.
p_k	The true (unknown) choice probability for alternative k.
$\hat{p}_k$	The empirical choice probability for alternative k.
$\mathcal{P}$	The ambiguity set for the true choice distribution.
η	The radius of the Kullback-Leibler divergence-based ambiguity set.
U_k	The utility for alternative k.
V_k	The deterministic component of utility for alternative k.
ε_k	The unobserved stochastic component of utility for alternative k.
t_k	The transformed variable for reformulation.

2.1. Problem definition

We adopt the conceptual foundation of the RUM [2, 27]. In this framework, the utility of alternative k is represented by the random variable $U_k = V_k + \varepsilon_k$. The decision-maker aims to maximize their utility by selecting an alternative from a choice set $\mathcal{K} := \{0, 1, \ldots, K\}$. The resulting maximum utility achieved by the decision-maker is:

$$\max_{k\in\mathcal{K}}\{U_k\}. \tag{2.1}$$

Here, $\mathcal{K}$ is the set of alternatives, with $k = 0$ often denoting a baseline. In most research, V_k is assumed to follow a parametric form (e.g., linear) based on observable attributes, leading to models like logit or probit [28, 29]. However, assuming a fixed functional form can be restrictive, and collecting attribute data for estimating the utility function may be impractical. To address these limitations, we propose a framework that learns preferences from choice data without imposing strong structural assumptions on the deterministic utility part V_k, instead linking it directly to choice probabilities.

2.1.1. Modeling preference uncertainty

Let p_k denote the true probability that the decision-maker chooses alternative $k \in \mathcal{K}$, forming the vector $\mathbf{p} = (p_0, \ldots, p_K)^\top$, which satisfies $p_k \geq 0$ and $\sum_{k\in\mathcal{K}} p_k = 1$. This vector $\mathbf{p}$ defines the decision-maker's true preference distribution $\mathbb{P}$ over $\mathcal{K}$, which is unknown. We estimate $\mathbb{P}$ from N historical choice outcomes $\{\xi_n\}_{n=1}^N$. The empirical probability of choosing k is:

$$\hat{p}_k = \frac{1}{N}\sum_{n=1}^{N}\mathbf{1}(\xi_n = k), \quad \forall k \in \mathcal{K}, \tag{2.2}$$

where $\mathbf{1}(\cdot)$ denotes the indicator function. These form the empirical probability distribution $\hat{\mathbb{P}}_N$, defined by the vector $\hat{\mathbf{p}} = (\hat{p}_0, \ldots, \hat{p}_K)^\top$, where $\hat{\mathbb{P}}_N$ is an estimate of $\mathbb{P}$. We assume that the historical choice data are exogenous, i.e., the generating process of the choice data are independent of the decision problem considered. This assumption is appropriate for scenarios where the decision-maker makes strategic decisions using historical data from a different and stable environment, or where the preference data are collected through controlled experiments. We define the Kullback-Leibler (KL) divergence-based ambiguity set $\mathcal{P}$ around $\hat{\mathbb{P}}_N$:

$$\mathcal{P} := \left\{\mathbb{P} \in \mathcal{M}(\mathcal{K}) : D\left(\mathbb{P}\|\hat{\mathbb{P}}_N\right) \leq \eta\right\}, \tag{2.3}$$

where $\mathcal{M}(\mathcal{K})$ is the set of distributions on $\mathcal{K}$, $\eta \geq 0$ is the radius, and $D(\cdot\|\cdot)$ is the KL divergence:

$$D\left(\mathbb{P}\|\hat{\mathbb{P}}_N\right) = \sum_{k\in\mathcal{K}} p_k \log\frac{p_k}{\hat{p}_k}. \tag{2.4}$$

To ensure that the KL divergence in (2.3) is well-defined, the empirical probability distribution $\hat{p}$ must be strictly positive. Under this condition, the ambiguity set $\mathcal{P}$ contains all probability distributions $\mathbb{P}$ considered plausible and sufficiently close to the empirical observations $\hat{\mathbb{P}}_N$.

Remark 1. In many practical datasets, some alternatives may never be chosen, leading to empirical probabilities $\hat{p}_k = 0$ for some k. To address this practical issue, we employ a standard regularization technique known as Laplace smoothing [30]. Instead of calculating $\hat{p}_k = \frac{N_k}{N}$, where N_k is the number of times alternative k is chosen in a sample of size N, we compute the smoothed probability $\hat{p}_k^{\text{smooth}}$ as:

$$\hat{p}_k^{\text{smooth}} = \frac{N_k + \alpha}{N + \alpha(K+1)}, \tag{2.5}$$

where $\alpha > 0$ is a small smoothing parameter (e.g., $\alpha = 1$ for add-one smoothing), and $K + 1$ is the total number of alternatives. This technique effectively regularizes the empirical distribution by assigning a small, non-zero probability to unobserved alternatives. Throughout the rest of this paper, we denote this smoothed empirical probability vector as $\hat{p}$ and assume $\hat{p}_k > 0$ for all $k \in \mathcal{K}$.

We select the KL divergence to construct the ambiguity set because of its two advantages over alternative modeling approaches (e.g., Wasserstein-DRO, moment-based DRO, etc.). First, it admits a clear statistical interpretation, enabling the ambiguity set to be viewed as a confidence region around the empirical distribution $\hat{\mathbb{P}}_N$. Second, its logarithmic structure is crucial for the computational tractability of our model.

2.1.2. Decision-maker's sequential decision and outcome

Given the uncertain preferences $\mathbb{P} \in \mathcal{P}$, the decision-maker engages in a sequential decision process. In the first stage, the decision-maker selects a strategy $m \in \{1, \ldots, M\}$. This choice determines the probability vector $\theta^m = (\theta^m_0, \ldots, \theta^m_K)^\top$, where θ^m_k is the probability that alternative k becomes available in the second stage. The baseline alternative 0 is assumed to be always available (i.e., $\theta^m_0 = 1$) to avoid the situation that no choice can be chosen in the second stage. The actual set of available alternatives realized in the second stage, denoted $\mathcal{K}_m$, is therefore random, following the distribution defined by θ^m.

In the second stage, after the available set $\mathcal{K}_m$ is realized, the decision-maker observes the random utilities $\{U_k\}_{k \in \mathcal{K}_m}$ and chooses the alternative $k^* = \arg\max_{k \in \mathcal{K}_m} U_k$ to maximize their utility. The utility obtained from this second-stage choice is $\tilde{U}_m$:

$$\tilde{U}_m := \max_{k \in \mathcal{K}_m} U_k. \tag{2.6}$$

Note that $\tilde{U}_m$ is a random variable due to the randomness in $\mathcal{K}_m$ (governed by θ^m) and the randomness in U_k (from ε_k). Importantly, its distribution also depends on $\mathbb{P} \in \mathcal{P}$ because V_k is linked to $\mathbf{p}$ (as shown later in Proposition 2.1).

2.1.3. Distributionally robust optimization formulation

The overall decision making problem is to determine the optimal first-stage strategy m for the decision-maker, considering the ambiguity $\mathbb{P} \in \mathcal{P}$ and anticipating their own second-stage behavior. The decision-maker aims to maximize the expected second-stage utility $\tilde{U}_m$ robustly against the worst-case distribution in $\mathcal{P}$. This is formulated as:

$$\max_{m \in \{1,\ldots,M\}} \left\{ \min_{\mathbb{P} \in \mathcal{P}} \mathbb{E}^{\mathbb{P}} \left[\tilde{U}_m \right] \right\}, \tag{2.7}$$

where $\mathbb{E}^{\mathbb{P}}[\cdot]$ represents the expectation over the randomness in $\tilde{U}_m$. The inner minimization finds the worst-case expected utility for strategy m.

This formulation uses a standard DRO approach [31] to achieve robustness against preference ambiguity. While the decision-maker's decision process is sequential, the optimization problem (2.7) is solved at the beginning to find the optimal first-stage strategy. To help readers better understand the structure of the model, we also provide a diagram in Figure 1 that illustrates the two-stage decision process.

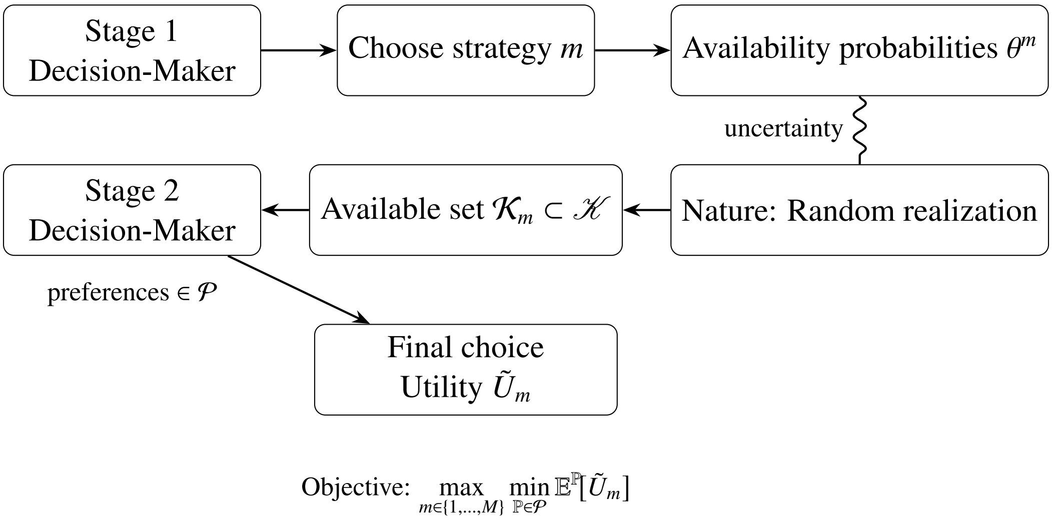

Figure 1. Schematic diagram of the proposed two-stage decision model for a single decision-maker.

2.1.4. Illustrative example

Now, we present an example to illustrate this framework from the decision-maker's perspective.

Example. Consider a decision-maker choosing enhancement projects from alternatives $\mathcal{K} = \{0, 1, 2, 3, 4\}$, where $k = 0$ is the baseline. In the first stage, the decision-maker selects a strategy m from the set $\{1, 2\}$. This strategy m determines the probability vector $\theta^m = (\theta_0^m, \ldots, \theta_K^m)^\top$, where θ_k^m for $k > 0$ is the probability that enhancement k is available in the second stage ($\theta_0^m = 1$). Let the strategies be defined by $\theta^1 = (1, 0.6, 0, 0.8, 0)^\top$ and $\theta^2 = (1, 0.4, 0.6, 0, 0.5)^\top$. For instance, under $m = 1$, alternatives $k = 1$ and $k = 3$ have probabilities 0.6 and 0.8 of being available, respectively, while $k = 2$ and 4 are unavailable. Consequently, when the decision-maker chooses m initially, the actual set of available alternatives in the second stage, denoted $\mathcal{K}_m$, is random and realized according to the probabilities in θ^m. The decision-maker does not know the exact composition of $\mathcal{K}_m$ when making the first-stage decision. Therefore, the decision-maker must choose m by anticipating their optimal utility-maximizing choice within the randomly realized set $\mathcal{K}_m$ while considering the ambiguity about their own preference distribution $\mathbb{P} \in \mathcal{P}$.

2.2. *Our problem vs classic random utility model*

In the classic RUM, the utility U_k that a decision-maker assigns to alternative $k \in \mathcal{K} = \{0, 1, \ldots, K\}$ is expressed as

$$U_k = V_k + \varepsilon_k, \tag{2.8}$$

where V_k represents the deterministic component of utility, often referred to as the representative utility, and ε_k captures the unobserved stochastic component. In most cases, the deterministic utility V_k is modeled as

$$V_k = \beta^T y_k, \tag{2.9}$$

where y_k is a vector of attributes associated with alternative k, and β denotes the decision-maker's preference weights for these attributes. In contrast, our approach circumvents the need for attribute data and associated parameter (β) estimation by representing V_k directly through choice probabilities (as detailed in Section 2.3). Furthermore, our model explicitly addresses uncertainty in decision-maker preferences through the ambiguity set $\mathcal{P}$ and uncertainty in future availability through the probability vectors θ^m.

2.3. Expected utility maximization

2.3.1. Uncertainty and distribution

The RUM addresses the problem of predicting the probability that a decision-maker chooses an alternative from a finite set of alternatives $\mathcal{K} = \{0, 1, \ldots, K\}$. Based on the definition in (2.8), we adopt the assumption from the most commonly used RUM, the multinomial logit (MNL) model, which posits that each ε_k follows an independently and identically distributed (i.i.d.) extreme value (Gumbel) distribution. This assumption ensures a closed-form expression for the choice probabilities, although alternative distributional assumptions can be considered and may lead to different model formulations.

To establish a direct link between the deterministic utility V_k and the choice probabilities p_k without relying on attributes, we leverage a foundational result from discrete choice theory. Under the i.i.d. Gumbel assumption, the probability of choosing alternative k is given by the well-known MNL formula, $p_k = e^{V_k} / \sum_{l \in \mathcal{K}} e^{V_l}$ [32]. By inverting this relationship and setting $V_0 = 0$ as a benchmark, we can express V_k directly in terms of the choice probabilities. This classic result enables us to obtain the distribution of U_k as follows.

Proposition 2.1. *Given $p = (p_0, p_1, \ldots, p_K)^\top$ with the deterministic part of utility for alternative* 0 *being the benchmark for all alternatives, i.e., $V_0 = 0$, and $\varepsilon_0, \varepsilon_1, \ldots, \varepsilon_K \overset{iid}{\sim} Gumbel(0, 1)$, then we have that for each $k \in \mathcal{K}$,*

$$V_k = \ln\left(\frac{p_k}{p_0}\right), \tag{2.10}$$

and

$$P(U_k \leq u) = e^{-\frac{p_k}{p_0} e^{-u}}. \tag{2.11}$$

2.3.2. Formulation

With the distribution specified in Proposition 2.1, the analytical form of the inner minimization problem can be obtained. This analysis relies on a foundational result for the expected maximum of Gumbel-distributed random variables, commonly known as the log-sum formula [32, 33]. As demonstrated in the following proposition, applying this result enables us to express the objective function in a closed form.

Proposition 2.2. *Given θ^m in the first stage and η as the bound on the KL divergence, the inner minimization problem of* (2.7) *can be formulated as follows:*

$$\begin{aligned} \min_{p_0,p_1,\ldots,p_K} \quad & \sum_{\mathcal{K}'\in\mathscr{K}} \prod_{k_1\in\mathcal{K}'} \theta^m_{k_1} \prod_{k_2\in\mathcal{K}\setminus\mathcal{K}'} (1-\theta^m_{k_2}) \left(\gamma + \ln \frac{\sum_{k\in\mathcal{K}'} p_k}{p_0}\right) \\ \text{s.t.} \quad & \sum_{k\in\mathcal{K}} p_k \log \frac{p_k}{\hat{p}_k} \le \eta, \\ & \sum_{k\in\mathcal{K}} p_k = 1, \\ & p_k \ge 0, \quad k \in \mathcal{K}, \end{aligned} \tag{2.12}$$

where $\hat{p}_k$ is the kth element in the distribution $\mathbb{P}_N$, estimated from historical observations defined in (2.2). *In addition, $\mathscr{K} = \{\mathcal{K}' \mid \mathcal{K}' \subseteq \mathcal{K}, \mathcal{K}' \neq \emptyset\}$ represents the set of all non-empty subsets of $\mathcal{K}$, and γ is the Euler–Mascheroni constant (as defined in Dence and Dence [34]).*

The results in Proposition 2.2 represent a reformulation of the inner problem in (2.7), where the objective function in (2.12) essentially reformulates $\mathbb{E}^{\mathbb{P}}\left[\tilde{U}_m\right]$ from (2.7). This reformulation calculates the worst-case expectation by explicitly summing the conditional expectations $\left(\gamma + \ln \frac{\sum_{k\in\mathcal{K}'} p_k}{p_0}\right)$ over all possible realizations $\mathcal{K}'$ of the available set, weighted by their probabilities $\left(\prod_{k_1\in\mathcal{K}'} \theta^m_{k_1} \prod_{k_2\in\mathcal{K}\setminus\mathcal{K}'}(1-\theta^m_{k_2})\right)$. Moreover, the terms $\prod_{k_1\in\mathcal{K}'} \theta^m_{k_1}$ and $\prod_{k_2\in\mathcal{K}\setminus\mathcal{K}'}(1-\theta^m_{k_2})$ represent the probabilities that, in the second stage, the alternatives in $\mathcal{K}'$ are available for the decision-maker to choose, while those in $\mathcal{K}\setminus\mathcal{K}'$ are absent, respectively.

A more detailed analysis of Proposition 2.2 is provided in the appendix. The most significant advantage of (2.12) is that, for fixed parameters θ^m and η in the first stage, the objective function in (2.12) is expressed as a linear combination of the term $\left(\gamma + \ln \frac{\sum_{k\in\mathcal{K}'} p_k}{p_0}\right)$.

Building on Proposition 2.2, we examine a nominal benchmark by setting the ambiguity radius $\eta = 0$. This represents a decision-maker who completely trusts the empirical data $\hat{\mathbb{P}}_N$. In this case, the only solution to the inner minimization problem (2.12) is $p_k = \hat{p}_k$ for all $k \in \mathcal{K}$. The utility for this nominal benchmark of a given strategy m is:

$$V^m_{\text{nominal}} = \sum_{\mathcal{K}'\in\mathscr{K}} \prod_{k_1\in\mathcal{K}'} \theta^m_{k_1} \prod_{k_2\in\mathcal{K}\setminus\mathcal{K}'} (1-\theta^m_{k_2}) \left(\gamma + \ln \frac{\sum_{k\in\mathcal{K}'} \hat{p}_k}{\hat{p}_0}\right). \tag{2.13}$$

The nominal benckmark utility represents the utility of strategy m without considering the ambiguity of preference.

3. Solution method

3.1. Problem reformulation

In this section, we reformulate the inner minimization problem (2.12) to facilitate further analysis. We introduce a variable transformation using unconstrained variables t_k to implicitly satisfy the probability constraints ($\sum p_k = 1, p_k > 0$). This transformation results in an equivalent optimization problem expressed in terms of these new variables.

To introduce the notation, we define $K+1$ new variables $t_0, t_1 \ldots, t_K$ where $t_k \in (-\infty, +\infty)$ for $k \in \mathcal{K}$. These variables are collectively denoted as $t = (t_0, t_1, \ldots, t_K)$ and $p_k(t) = \frac{e^{t_k}}{\sum_{l\in\mathcal{K}} e^{t_l}}$. Now, for these new decision variables, the following conditions are satisfied:

$$\begin{cases} \sum_{k\in\mathcal{K}} \dfrac{e^{t_k}}{\sum_{l\in\mathcal{K}} e^{t_l}} = 1, \\ \dfrac{e^{t_k}}{\sum_{l\in\mathcal{K}} e^{t_l}} > 0,\ k \in \mathcal{K}. \end{cases} \tag{3.1}$$

From the definition in (3.1), we have that $p_k(t)$ is positive, which can approach a very small positive value close to zero. By incorporating t, we can reformulate (2.12) as

$$\begin{aligned} \min_{t_0,t_1,\ldots,t_K} \quad & \sum_{\mathcal{K}'\in\mathscr{K}} \prod_{k_1\in\mathcal{K}'} \theta_{k_1}^m \prod_{k_2\in\mathcal{K}\setminus\mathcal{K}'} (1-\theta_{k_2}^m)\left(\gamma + \ln \frac{\sum_{k\in\mathcal{K}'} e^{t_k}}{e^{t_0}}\right) \\ \text{s.t.} \quad & \sum_{k\in\mathcal{K}} \frac{e^{t_k}}{\sum_{l\in\mathcal{K}} e^{t_l}} \log \frac{\frac{e^{t_k}}{\sum_{l\in\mathcal{K}} e^{t_l}}}{\hat{p}_k} \le \eta, \\ & t_k \in \mathbb{R},\ k \in \mathcal{K}. \end{aligned} \tag{3.2}$$

Based on the above reformulation, we analyze the convexity of this problem.

3.2. Convexity

We analyze the convexity of the objective function $f(t)$ and the constraint function $c(t)$ defined below. We show that $f(t)$ is convex and $c(t)$ is convex under certain conditions on the probabilities $p_k(t)$. Incorporating these conditions leads to a convex optimization problem.

$$f(t_0, t_1, \ldots, t_K) := \sum_{\mathcal{K}'\in\mathscr{K}} \prod_{k_1\in\mathcal{K}'} \theta_{k_1}^m \prod_{k_2\in\mathcal{K}\setminus\mathcal{K}'} (1-\theta_{k_2}^m)\left(\gamma + \ln \frac{\sum_{k\in\mathcal{K}'} e^{t_k}}{e^{t_0}}\right), \tag{3.3}$$

$$c(t_0, t_1, \ldots, t_K) := \sum_{k\in\mathcal{K}} \frac{e^{t_k}}{\sum_{l\in\mathcal{K}} e^{t_l}} \log \frac{\frac{e^{t_k}}{\sum_{l\in\mathcal{K}} e^{t_l}}}{\hat{p}_k} - \eta. \tag{3.4}$$

Proposition 3.1. *The function $f(t_0, t_1, \ldots, t_K)$ is convex in $t = (t_0, t_1, \ldots, t_K) \in \mathbb{R}^{K+1}$.*

Next, we investigate the convexity of $c(t_0, t_1, \ldots, t_K)$. To this end, we first present two auxiliary lemmas:

Lemma 3.1. *If $e^{t_i}\left(\sum_{l=0}^{K} e^{t_l}\right)^{-1} < \frac{1}{2}$, the function*

$$g_i(t) = \frac{e^{t_i}}{\sum_{l=0}^{K} e^{t_l}} \tag{3.5}$$

is convex with respect to $t = (t_0, t_1, \ldots, t_K) \in \mathbb{R}^{K+1}$ for all $i \in \{0, \ldots, K\}$.

Lemma 3.2. *The function $\psi(x) = x \ln \frac{x}{a}$ is convex with respect to x for $a \in (0, 1)$. Furthermore, $\psi(x)$ is decreasing on $(0, \frac{a}{e})$ and increasing on $(\frac{a}{e}, +\infty)$.*

Using these lemmas, we establish the convexity of $c(t_0, t_1, \ldots, t_K)$ under specific conditions:

Proposition 3.2. *For all $k \in \mathcal{K}$, if the following condition holds:*

$$\frac{\hat{p}_k}{e} \leq \frac{e^{t_k}}{\sum_{l \in \mathcal{K}} e^{t_l}} \leq \frac{1}{2}, \quad \forall k \in \mathcal{K}, \tag{3.6}$$

then function $c(t_0, t_1, \ldots, t_K)$ is convex in $t = (t_0, t_1, \ldots, t_K) \in \mathbb{R}^{K+1}$.

The proofs of these results are provided in the appendix. Based on the above results, we conclude that the following problem is convex:

$$\begin{aligned}
\min_{t_0, t_1, \ldots, t_K} \quad & \sum_{\mathcal{K}' \in \mathscr{K}} \prod_{k_1 \in \mathcal{K}'} \theta_{k_1}^m \prod_{k_2 \in \mathcal{K} \setminus \mathcal{K}'} (1 - \theta_{k_2}^m) \left(\gamma + \ln \frac{\sum_{k \in \mathcal{K}'} e^{t_k}}{e^{t_0}} \right) \\
\text{s.t.} \quad & \sum_{k \in \mathcal{K}} \frac{e^{t_k}}{\sum_{l \in \mathcal{K}} e^{t_l}} \log \frac{\frac{e^{t_k}}{\sum_{l \in \mathcal{K}} e^{t_l}}}{\hat{p}_k} \leq \eta, \\
& \frac{\hat{p}_k}{e} \leq \frac{e^{t_k}}{\sum_{l \in \mathcal{K}} e^{t_l}} \leq \frac{1}{2}, \ k \in \mathcal{K}, \\
& t_k \in \mathbb{R}, \ k \in \mathcal{K}.
\end{aligned} \tag{3.7}$$

Compared to (3.2) or equivalently (2.12) in Proposition 2.2, a set of additional constraints is added to the above optimization problem. Here, we provide clarifications for these additional constraints.

Remark 2. We provide justifications for the additional constraints on p_i. The lower bound on p_i can be interpreted as an assumption of preference stability. In decision theory, a decision-maker's preference is typically assumed to be relatively stable over a short time period. This condition prevents the true preference p_i from deviating too much from the empirical observation $\hat{p}_i$. Its practical implication is to focus the model on stable preference patterns. The upper bound on p_i can be interpreted as a constraint on the preference for a particular alternative does not significantly outweigh that of all others when considering multiple alternatives. If one alternative has a choice probability significantly greater than $\frac{1}{2}$, the decision problem is simplified to a heuristic that always maximizes the availability of that alternative. Our framework is designed for the more complex and common scenario where a meaningful trade-off exists among several viable alternatives.

3.3. Augmented lagrangian method

3.3.1. Augmented lagrangian function

In this section, we investigate an augmented Lagrangian method (ALM) [35–37] to solve problem (3.7). We introduce a set of slack variables $s, r_k, o_k, k \in \mathcal{K}$ as follows:

$$
\begin{aligned}
\min_{t,s,r,o} \quad & \sum_{\mathcal{K}' \in \mathscr{K}} \prod_{k_1 \in \mathcal{K}'} \theta^m_{k_1} \prod_{k_2 \in \mathcal{K} \setminus \mathcal{K}'} (1 - \theta^m_{k_2}) \left(\gamma + \ln \frac{\sum_{k \in \mathcal{K}'} e^{t_k}}{e^{t_0}} \right) \\
\text{s.t.} \quad & \sum_{k \in \mathcal{K}} \frac{e^{t_k}}{\sum_{l \in \mathcal{K}} e^{t_l}} \log \frac{\frac{e^{t_k}}{\sum_{l \in \mathcal{K}} e^{t_l}}}{\hat{p}_k} - \eta + s = 0, \\
& \frac{\hat{p}_k}{e} - \frac{e^{t_k}}{\sum_{l \in \mathcal{K}} e^{t_l}} + r_k = 0, \ k \in \mathcal{K}, \\
& \frac{e^{t_k}}{\sum_{l \in \mathcal{K}} e^{t_l}} - \frac{1}{2} + o_k = 0, \ k \in \mathcal{K}, \\
& t_k \in \mathbb{R}, s, r_k, o_k \geq 0, \ k \in \mathcal{K}.
\end{aligned} \tag{3.8}
$$

We further denote $r = (r_0, r_1, \ldots, r_K)^\top$ and $o = (o_0, o_1, \ldots, o_K)^\top$, and let

$$
\begin{aligned}
c_s(t) \ &:= \ \sum_{k \in \mathcal{K}} \frac{e^{t_k}}{\sum_{l \in \mathcal{K}} e^{t_l}} \log \frac{\frac{e^{t_k}}{\sum_{l \in \mathcal{K}} e^{t_l}}}{\hat{p}_k} - \eta, \\
c_r^k(t) \ &:= \ \frac{\hat{p}_k}{e} - \frac{e^{t_k}}{\sum_{l \in \mathcal{K}} e^{t_l}}, \\
c_o^k(t) \ &:= \ \frac{e^{t_k}}{\sum_{l \in \mathcal{K}} e^{t_l}} - \frac{1}{2}.
\end{aligned} \tag{3.9}
$$

Based on the notations above, we define the Lagrangian function as follows:

$$
L(t, s, r, o, \mu) = f(t) + \mu_s(c_s(t) + s) + \sum_{k \in \mathcal{K}} \mu_r^k (c_r^k(t) + r_k) + \sum_{k \in \mathcal{K}} \mu_o^k (c_o^k(t) + o_k), \tag{3.10}
$$

for $s, r_k, o_k \geq 0, \ k \in \mathcal{K}$, and $f(t)$ defined in (3.3). The quadratic penalty function of the problem above is

$$
p(t, s, r, o) = (c_s(t) + s)^2 + \sum_{k \in \mathcal{K}} (c_r^k(t) + r_k)^2 + \sum_{k \in \mathcal{K}} (c_o^k(t) + o_k)^2, \tag{3.11}
$$

and the augmented Lagrangian function with penalty factor σ is

$$
L_\sigma(t, s, r, o, \mu) = f(t) + \mu_s(c_s(t) + s) + \sum_{k \in \mathcal{K}} \mu_r^k (c_r^k(t) + r_k) + \sum_{k \in \mathcal{K}} \mu_o^k (c_o^k(t) + o_k) + \frac{\sigma}{2} p(t, s, r, o), \tag{3.12}
$$

for $s, r_k, o_k \geq 0, \ k \in \mathcal{K}$.

3.3.2. Algorithm

Now we proceed to an iterative algorithm to solve the problem. Given that at iteration j, the multiplier and the penalty factor in (3.12) are μ^j and σ_j, respectively. We need to solve the following optimization problem:

$$
\min_{t,s,r,o} L_{\sigma_j}(t, s, r, o, \mu^j), \quad \text{s.t. } s, r_k, o_k \geq 0, \ k \in \mathcal{K}. \tag{3.13}
$$

This updates the decision and slack variables t, s, r_k, o_k at iteration $j+1$, denoted by $t^{j+1}, s^{j+1}, r_k^{j+1}, o_k^{j+1}$ for each $k \in \mathcal{K}$. In fact, the optimization problem (3.13) can be simplified by focusing on the variable t. First, given a fixed value of t, the subproblem with respect to s, r, and o can be formulated as:

$$\min_{s,r_k,o_k\geq 0} \mu_s(c_s(t) + s) + \sum_{k\in\mathcal{K}} \mu_{r_k}(c_{r_k}(t) + r_k) + \sum_{k\in\mathcal{K}} \mu_{o_k}(c_{o_k}(t) + o_k) + \frac{\sigma_j}{2} p(t, s, r, o). \tag{3.14}$$

Due to the convexity of (3.14), s, r and o are the global optima of the problem if and only if

$$\begin{aligned} s &= \max\left\{-\frac{\mu_s}{\sigma_j} - c_s(t), 0\right\}, \\ r_k &= \max\left\{-\frac{\mu_{r_k}}{\sigma_j} - c_{r_k}(t), 0\right\}, \\ o_k &= \max\left\{-\frac{\mu_{o_k}}{\sigma_j} - c_{o_k}(t), 0\right\}. \end{aligned} \tag{3.15}$$

By substituting s, r, o into $L_{\sigma_j}(t, s, r, o, \mu^j)$, we have

$$\begin{aligned} \check{L}_{\sigma_j}(t, \mu^j) = f(t) &+ \frac{\sigma_j}{2}\left\{\left[\max\{\frac{\mu_s}{\sigma_j} + c_s(t), 0\}\right]^2 - \frac{\mu_s^2}{\sigma_j^2}\right\} + \frac{\sigma_j}{2}\sum_{k\in\mathcal{K}}\left\{\left[\max\{\frac{\mu_{r_k}}{\sigma_j} + c_{r_k}(t), 0\}\right]^2 - \frac{\mu_{r_k}^2}{\sigma_j^2}\right\} \\ &+ \frac{\sigma_j}{2}\sum_{k\in\mathcal{K}}\left\{\left[\max\{\frac{\mu_{o_k}}{\sigma_j} + c_{o_k}(t), 0\}\right]^2 - \frac{\mu_{o_k}^2}{\sigma_j^2}\right\}. \end{aligned} \tag{3.16}$$

Therefore, (3.13) is equivalent to

$$\min_{t\in\mathbb{R}^{K+1}} \check{L}_{\sigma_j}(t, \mu^j). \tag{3.17}$$

Due to the continuous differentiability of the solution to (3.16), the above optimization problem can be solved using the gradient descent method.

We propose the following framework to achieve $t^{j+1}, s^{j+1}, r_k^{j+1}$ and o_k^{j+1} for $k \in \mathcal{K}$ in iteration $j + 1$. On one hand, we examine the optimal condition for (3.8), where optimal solutions t^*, s^*, r^*, o^* and multiplier μ^* satisfy the following Karush-Kuhn-Tucker (KKT) conditions:

$$\begin{aligned} 0 &= \nabla f(t^*) + \mu_s^*\nabla c_s(t^*) + \sum_{k\in\mathcal{K}} \mu_{r_k}^*\nabla c_{r_k}(t^*) + \sum_{k\in\mathcal{K}} \mu_{o_k}^*\nabla c_{o_k}(t^*), \\ \mu_s^* &\geq 0, \\ s^* &\geq 0, \\ \mu_{r_k}^* &\geq 0,\ k \in \mathcal{K}, \\ r_k^* &\geq 0,\ k \in \mathcal{K}, \\ \mu_{o_k}^* &\geq 0,\ k \in \mathcal{K}, \\ o_k^* &\geq 0,\ k \in \mathcal{K}. \end{aligned} \tag{3.18}$$

On the other hand, for the optimization problem (3.13), the solutions $t^{j+1}, s^{j+1}, r^{j+1}, o^{j+1}$ satisfy the following KKT conditions:

$$
\begin{aligned}
0 &= \nabla f(t^{j+1}) + \left(\mu_s^j + \sigma_j(c_s(t^{j+1}) + s^{j+1})\right) \nabla c_s(t^{j+1}) \\
&\quad + \sum_{k\in\mathcal{K}} \left(\mu_{r_k}^j + \sigma_j(c_{r_k}(t^{j+1}) + r_k^{j+1})\right) \nabla c_{r_k}(t^{j+1}) \\
&\quad + \sum_{k\in\mathcal{K}} \left(\mu_{o_k}^j + \sigma_j(c_{o_k}(t^{j+1}) + o_k^{j+1})\right) \nabla c_{o_k}(t^{j+1}), \\
s^{j+1} &= \max\left\{-\frac{\mu_s^j}{\sigma_j} - c_s(t^{j+1}), 0\right\}, \\
r_k^{j+1} &= \max\left\{-\frac{\mu_{r_k}^j}{\sigma_j} - c_{r_k}(t^{j+1}), 0\right\},\ k \in \mathcal{K}, \\
o_k^{j+1} &= \max\left\{-\frac{\mu_{o_k}^j}{\sigma_j} - c_{o_k}(t^{j+1}), 0\right\},\ k \in \mathcal{K}.
\end{aligned}
\tag{3.19}
$$

By comparing such two KKT conditions above, the update formula for multiplier μ can be derived as:

$$
\begin{aligned}
\mu_s^{j+1} &= \max\left\{\mu_s^j + \sigma_j c_s(t^{j+1}), 0\right\}, \\
\mu_{r_k}^{j+1} &= \max\left\{\mu_{r_k}^j + \sigma_j c_{r_k}(t^{j+1}), 0\right\}, \\
\mu_{o_k}^{j+1} &= \max\left\{\mu_{o_k}^j + \sigma_j c_{o_k}(t^{j+1}), 0\right\},
\end{aligned}
\tag{3.20}
$$

where t^{j+1} is the optimal solution to problem (3.17). Regarding the equality constraints in (3.8), we introduce the following function to measure the violation of these constraints,

$$
v_j(t^{j+1}) = \sqrt{(c_s(t^{j+1}) + s^{j+1})^2 + \sum_{k\in\mathcal{K}} \left(c_{r_k}(t^{j+1}) + r_k^{j+1}\right)^2 + \sum_{k\in\mathcal{K}} \left(c_{o_k}(t^{j+1}) + o_k^{j+1}\right)^2}. \tag{3.21}
$$

By substituting the results of (3.15) into (3.21), we can further rewrite $v_j(t^{j+1})$ as:

$$
\begin{aligned}
v_j(t^{j+1}) &= \\
&\sqrt{\left(\max\left\{c_s(t^{j+1}), -\frac{\mu_s^j}{\sigma_j}\right\}\right)^2 + \sum_{k\in\mathcal{K}} \left(\max\left\{c_{r_k}(t^{j+1}), -\frac{\mu_{r_k}^j}{\sigma_j}\right\}\right)^2 + \sum_{k\in\mathcal{K}} \left(\max\left\{c_{o_k}(t^{j+1}), -\frac{\mu_{o_k}^j}{\sigma_j}\right\}\right)^2}.
\end{aligned}
\tag{3.22}
$$

The pseudo-code of presented Algorithm 1 is provided in Appendix B, and the key steps of the algorithm are summarized as follows:

1. Initialization: Initialize the iteration counter $j = 0$, the multipliers μ^0, and the penalty parameter σ^0.

2. Subproblem solution: Solve the unconstrained subproblem for the transformed variables t^{j+1}:

$$
t^{j+1} = \arg\min_{t\in\mathbb{R}^{K+1}} \check{L}_{\sigma_j}(t, \mu^j), \tag{3.23}
$$

where $\check{L}_{\sigma_j}(t, \mu^j)$ is the augmented Lagrangian function defined in (3.17). This minimization is performed using a gradient-based optimization method.

3. Multiplier update: Update the Lagrange multipliers using the results from the subproblem solution. Following the standard ALM update rule, the new multipliers μ^{j+1} are computed via the following formula:

$$\mu^{j+1} = \max\{\mu^j + \sigma_j c(t^{j+1}), 0\}, \tag{3.24}$$

where $c(t^{j+1})$ represents the vector of constraint violations at t^{j+1}.

4. Penalty parameter update: The penalty parameter σ_j is adaptively increased to encourage feasibility. If the constraint violation does not decrease sufficiently compared to the previous iteration, we update $\sigma_{j+1} = \rho \cdot \sigma_j$ for some $\rho > 1$; otherwise, $\sigma_{j+1} = \sigma_j$.

5. Convergence check: The algorithm terminates if either a feasibility condition or an optimality condition is met. The iteration stops if the constraint violation $v_j(t^{j+1})$ (defined in (3.22)) falls below a feasibility tolerance, or if the relative change in the objective function value between consecutive iterations falls below an optimality tolerance. The algorithm also terminates if a maximum number of iterations is reached.

Parameter selection Our implementation of the ALM involves several key hyperparameters. For the main ALM procedure, we set the initial Lagrange multipliers $\mu^0 = 100$ and the initial penalty parameter $\sigma_0 = 40$. The penalty parameter is adaptively increased by a growth factor of $\rho = 2$ if feasibility is not sufficiently improved in an iteration. The algorithm terminates when the constraint violation falls below a feasibility tolerance of $\varepsilon = 10^{-6}$.

The unconstrained subproblem in each ALM iteration is solved using the RMSprop optimizer [38]. The RMSprop hyperparameters are set as follows: The learning rate is 10^{-3}, the momentum factor is $\gamma = 0.9$, and a numerical stability constant of $\varepsilon_{num} = 10^{-8}$ is used. The inner optimization is terminated after a maximum of 2000 iterations.

Computational complexity The main computational cost of the proposed ALM lies in the iterative solution of the unconstrained subproblem (3.17). The objective function in this subproblem contains a summation over all $2^{K+1} - 1$ non-empty subsets of the $K + 1$ alternatives. Consequently, each evaluation of the objective function and its gradient, which is required at each step of the inner gradient-based solver, has a computational complexity of $O(2^K)$.

In contrast, all other operations within each ALM iteration, such as the updates for the Lagrange multipliers and the penalty parameter, are computationally inexpensive, which is $O(K)$. Therefore, the overall complexity of the algorithm is dominated by the subproblem solution, which scales exponentially with the number of alternatives.

4. Numerical examples

The numerical examples consist of four subsections. First, we present a case study of a supply chain management problem. Second, we conduct a sensitivity analysis of the hyperparameters. Third, we examine how the uncertainty radius and strategy structure influence the results. Finally, we evaluate the computational performance of the algorithm.

To align with the two-stage framework, the experimental data are generated in two steps. First, we simulate historical choice records for the decision-maker across various alternatives to represent the choice probabilities. Second, we generate historical availability records for each alternative to capture the availability probabilities.

To further demonstrate the practical credibility of the proposed framework, we provide a real-world project investment case study in Appendix C. This case supplements the synthetic experiments by incorporating a real industrial decision scenario.

4.1. Supplier selection problem

A company seeks to optimize its procurement strategy by selecting one of five suppliers to replenish inventory of a critical component and mitigate potential shortages. There are nine alternatives ($\mathcal{K} = \{0, \ldots, 8\}$), comprising eight distinct components plus a baseline (Alternative 0). Historical data yield empirical selection probabilities for these alternatives, denoted as $\hat{\mathbf{p}} = (\hat{p}_0, \ldots, \hat{p}_8)^\top$ (Table 2). The empirical probabilities $\hat{p}$ used in our experiments are computed from the simulated historical data after applying Laplace smoothing with $\alpha = 1$. In addition, five suppliers can produce these alternatives, and their corresponding probabilities for on-time delivery are detailed in Table 3. The baseline alternative is assumed to be reliably delivered by all suppliers.

Table 2. The set of alternatives and their synthetic selection probabilities ($\hat{p}$) for the Supplier Selection Problem.

Alternative No.	**0**	**1**	**2**	**3**	**4**	**5**	**6**	**7**	**8**
Empirical Selection Prob. ($\hat{p}$)	2%	12%	15%	20%	10%	8%	11%	17%	5%

Table 3. The synthetic on-time provision probabilities (θ_k^m) for each alternative under each of the five suppliers.

Alternative	**Supplier**				
No.	**1**	**2**	**3**	**4**	**5**
0	100%	100%	100%	100%	100%
1	85%	0%	84%	78%	88%
2	75%	68%	66%	61%	90%
3	90%	74%	0%	70%	0%
4	65%	0%	72%	0%	95%
5	0%	62%	0%	0%	92%
6	0%	80%	0%	52%	0%
7	0%	50%	78%	67%	0%
8	0%	0%	70%	0%	81%

The optimal solutions are derived by solving (3.7) using the corresponding parameters for the suppliers outlined in Table 3. The utilities in Table 4 represent the expected worst-case utilities that the company can achieve in the second stage. It is noted that Supplier 4 offers the maximum worst-case utility and is consequently selected in the first stage. The optimal values for these five suppliers range from 1.460 to 1.570.

The first column in Table 3 lists the alternatives, ranging from 0 to 8. The subsequent columns present the capabilities of the suppliers. For example, the second column provides the capability of Supplier 1 to provide each alternative, where the 100% in the first row indicates that Alternative 0 is the baseline alternative, meaning that the delivery within the deadline of this alternative can be guaranteed by all suppliers. In each column, the values indicate the probabilities that the corresponding supplier will deliver the respective alternatives on time.

Table 4. The optimal worst-case expected utility for each of the five suppliers, computed with an ambiguity radius of $\eta = 0.1$ using synthetic data.

Supplier	1	2	3	4	5
Utility	1.489	1.524	1.460	1.570	1.469

In Figure 2, we illustrate the convergence behavior of the algorithm for each of the five suppliers. The values of the objective function for each supplier stabilize within a small number of iterations, indicating that the algorithm converges efficiently in practice. This rapid stabilization is theoretically supported by the convex structure of the problem and is consistent with the convergence behavior of ALMs for convex optimization [39].

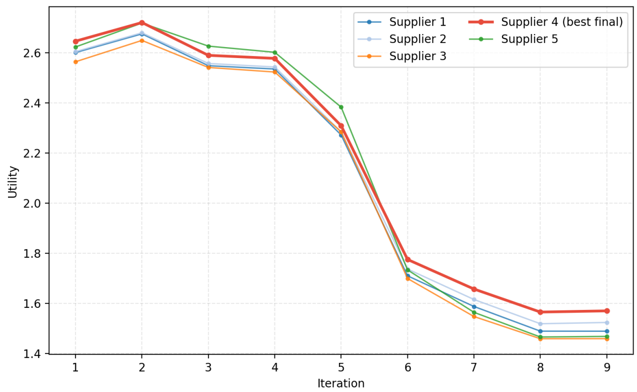

Figure 2. Convergence of the worst-case expected utility for the five suppliers under an ambiguity radius of $\eta = 0.1$.

These results indicate the practical efficiency of the algorithm and motivate a further examination of how its convergence behavior may vary with different hyperparameter choices.

4.2. Sensitivity analysis of hyperparameters

We perform a set of numerical tests for comparative analysis on how the initial multiplier μ^0 and the initial penalty factor σ_0 influence the solution. To facilitate a clearer analysis of hyperparameter effects, we employ a smaller illustrative example. For this analysis, we consider a scenario with four alternatives (indexed 0 to 3) available in the second stage, alongside the baseline Alternative 0, which is always available. The empirical selection probabilities for these alternatives are given as $\hat{p} = (1\%,\ 48\%,\ 30\%,\ 21\%)^\top$. In this context, there are $M = 3$ first-stage strategies for the decision-maker to choose in the first stage. The corresponding probabilities (θ_k^m) that these alternatives will be available in the second stage under strategy $m \in \{1, 2, 3\}$ are presented in Table 5. Columns 2 through 4 present the probabilities for θ^1, θ^2, and θ^3, respectively, while the first column lists the alternatives. Alternative 0 has $\theta_0^m = 100\%$ for all m.

Table 5. The three first-stage strategy structures ($\theta^1, \theta^2, \theta^3$) used in the small-scale example for hyperparameter sensitivity analysis.

Alternative	Strategy		
No.	θ^1	θ^2	θ^3
0	100%	100%	100%
1	30%	55%	0%
2	70%	0%	90%
3	0%	80%	60%

We begin by solving for the different strategies ($\{\theta^m\}_{m=1,2,3}$) using the original hyperparameter settings to identify the optimal option.

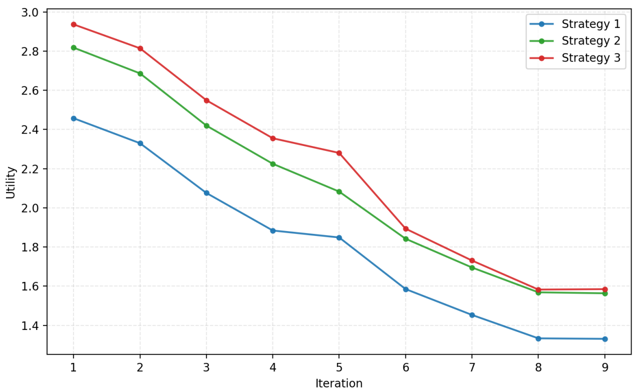

Figure 3. Convergence of the worst-case expected utility for the three strategies defined in the hyperparameter sensitivity analysis, computed with ambiguity radius $\eta = 0.1$ using synthetic data.

Table 6. Original hyperparameter settings and the ranges used for the sensitivity analysis of the initial multiplier (μ^0) and the initial penalty factor (σ_0).

No.	Hyperparameter	Original Setting	Value to Test
1	μ^0 (initial multiplier)	100	{2, 5, 10, 20, 50, 200}
2	σ_0 (initial penalty factor)	40	{4, 8, 20, 80, 200, 400}

Figure 3 illustrates the convergence of the simple example provided, and Strategy 3 is the best choice in the first stage. The figure also demonstrates that the differences between iterates are significantly reduced after a small number of iterations. To further analyze the solution, we conduct tests to examine how the initial multiplier μ^0 and the initial penalty factor σ_0 influence the solution. We vary their values as outlined in Table 6 while using the value of θ^1 in Table 5 as the strategy structure. To simplify the analysis, we use the convergence process for Strategy 1 as a benchmark, which is illustrated in Figure 3. First, we perform a set of numerical tests for the initial multiplier μ^0, varying its values among 2%, 5%, 10%, 20%, 50%, and 200% of the original setting of 100, as shown in Table 6. Figure 4 presents the convergences for varying values of μ^0.

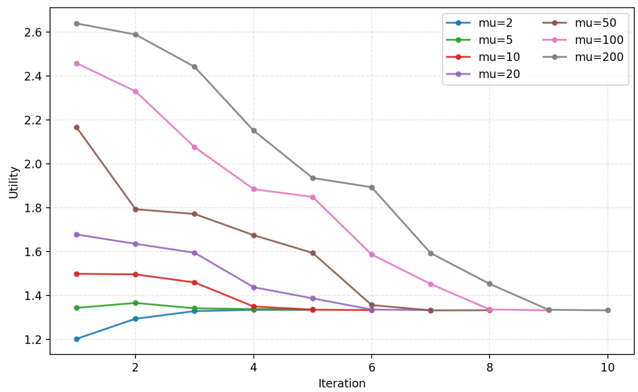

Figure 4. Convergence behavior of the algorithm for Strategy 1 under different values of the initial multiplier μ^0, computed with ambiguity radius $\eta = 0.1$ using synthetic data.

Second, we proceed to analyze how the value of the initial penalty factor σ_0 influences the numerical results. For this analysis, we consider values of σ_0 at 10%, 20%, 50%, 200%, 500%, and 1,000% of the original value of 40, resulting in the corresponding test set: $\{4, 8, 20, 80, 200, \text{and } 400\}$, respectively. Figure 5 illustrates the significantly different convergence behaviors for these varying values of σ_0.

The investigation into varying the values of μ^0 reveals that different hyperparameters lead to distinct convergence behaviors. In particular, Figure 4 shows that the differences in each case are caused by the impact of μ^0 on the solution of the subproblem in each iteration. It is worth mentioning that when $\mu^0 = 2$, the objective function value initially *increases* along the growth of the iterations. Analysis of the algorithm's execution reveals that the solutions obtained in the first and second iterations violate feasibility constraints, indicating that $\mu^0 = 2$ is not an appropriate setting. Furthermore, the results in

Figure 4 demonstrate that a smaller value of the initial multiplier μ^0 leads to a higher probability of encountering infeasible values in the initial iterations of Algorithm 1. Similarly, Figure 5 illustrates that different initial values of σ_0 also yield distinct convergence behaviors. Figure 4 and Figure 5 also demonstrate that varying the hyperparameters μ^0 and σ_0 may result in a different number of iterations required for convergence.

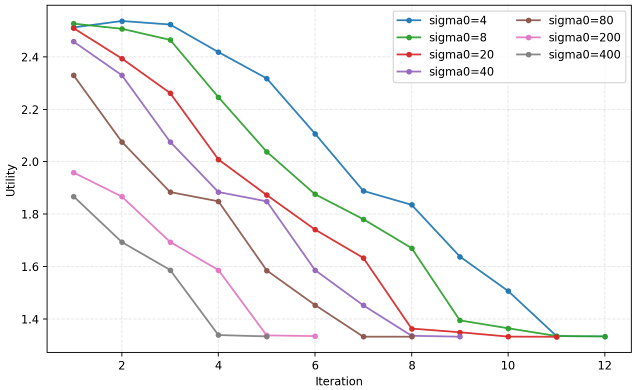

Figure 5. Convergence behavior of the algorithm for Strategy 1 under different values of the initial penalty factor σ_0, computed with ambiguity radius $\eta = 0.1$ using synthetic data.

4.3. Sensitivity analysis of ambiguity radius and strategy structures

To further investigate the properties of our proposed framework and address the selection of key parameters, we conduct a sensitivity analysis on two critical components, which are the ambiguity radius η and the structure of the first-stage strategies.

4.3.1. Sensitivity analysis of ambiguity radius η and robustness analysis

The ambiguity radius η quantifies the decision-maker's aversion to preference ambiguity. To understand its impact, we analyze the performance of the three strategies defined in Section 4.2 under a wide range of $\eta \in \{0.0, 0.01, 0.05, 0.1, 0.2, 0.5, 1.0, 5.0, 10.0, 20.0\}$. This analysis provides quantitative indicators of robustness, with the results presented in Figure 6. The yellow dashed line represents the optimal strategy under different η values, which is the upper envelope of the worst-case expected utilities for all strategies.

First, the worst-case expected utility serves as a primary robustness metric. As expected, Figure 6 shows that the worst-case expected utility for all strategies is monotonically decreasing in η. This illustrates the fundamental trade-off between robustness and performance that, as η increases, the robustness improves, while the guaranteed worst-case utility declines. Notably, a sharp initial drop in utility for $\eta = 0.01$ indicates the significant impact of introducing even a minor degree of preference uncertainty.

Second, the analysis reveals a clear shift in the optimal strategy. As shown by the upper envelope, the best strategy changes as the decision-maker's ambiguity aversion increases. In our experiment, Strategy 3 is optimal when $\eta \le 0.1$, but Strategy 2 becomes the best choice when $\eta \ge 0.5$. This demonstrates thatdifferent strategies are optimal for different risk preferences, and our framework provides a valuable tool for selecting the appropriate strategic choice based on the decision-maker's attitude toward ambiguity. We also compute the nominal benchmark utility for each of these strategies by (2.13). The results are illustrated in Table 7.

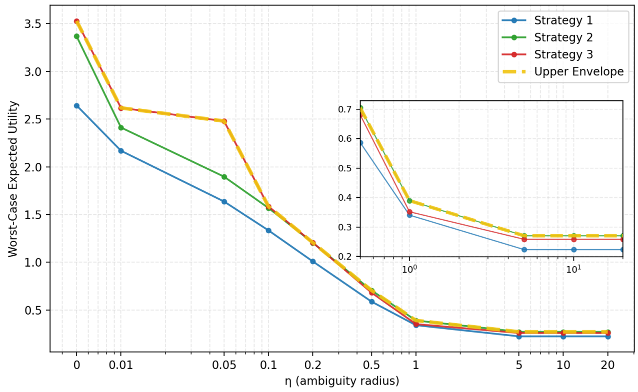

Figure 6. Sensitivity analysis of the worst-case expected utility with respect to the ambiguity radius η, computed using synthetic data.

From Table 7, we can see that the nominal benchmark utility for each strategy is greater than the worst-case expected utility when $\eta = 0$. This is because the worst-case expected utility is constrained by the additional constraints in (3.7), i.e., $\frac{\hat{p}_k}{e} \leq p_k \leq \frac{1}{2}$ and $k \in \mathcal{K}$. These constraints are instrumental for ensuring the convexity and tractability of our problem, but they are inherently restrictive. The gap between the nominal benchmark utility and the worst-case expected utility quantifies the price of tractability for ensuring a solvable convex problem.

Table 7. Comparison of the unconstrained Nominal Benchmark Utility versus the constrained Worst-Case Expected Utility at an ambiguity radius $\eta = 0$, computed using the synthetic data for the three strategies defined in Section 4.2.

Strategy	**Nominal benchmark utility**	**Worst-case expected utility**
1	3.5277	2.6427
2	3.9847	3.3680
3	4.1326	3.5282

4.3.2. Sensitivity analysis of strategy structures

In practice, a decision-maker may face different types of strategic choices. Some strategies might be 'specialized', focusing on making one or two alternatives that arehighly available, while others might be 'diversified', providing moderate availability across a broader range of options. We investigate how our model evaluates these strategy structures. We define four strategies as follows:

- Specialized strategies (Strategies 1–3): Each concentrates availability on a single alternative; e.g., $\theta^1 = (100\%, 99\%, 0\%, 0\%)$, $\theta^2 = (100\%, 0\%, 99\%, 0\%)$, and $\theta^3 = (100\%, 0\%, 0\%, 99\%)$. This corresponds to committing to one dominant option.

- Diversified strategy (Strategy 4): Distributes availability across alternatives, representing a hedging choice, e.g., $\theta^4 = (100\%, 40\%, 40\%, 40\%)$.

We compute the worst-case expected utility for each of these four strategies across the same range of η values. The results are illustrated in Figure 7.

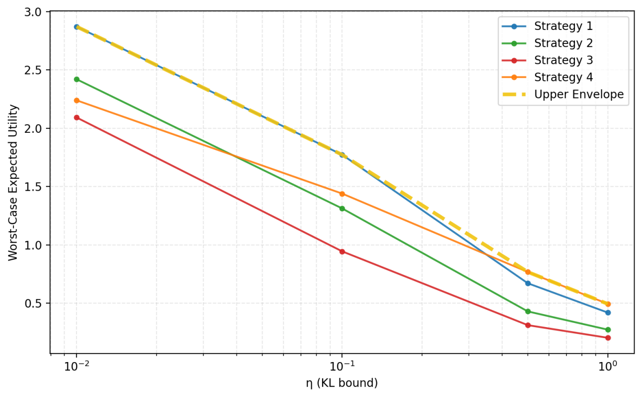

Figure 7. Performance comparison of specialized versus diversified strategy structures under varying ambiguity radius η, computed using synthetic data.

Figure 7 illustrates how the optimal strategy shifts as η increases. When $\eta \leq 0.1$, Strategy 1 is optimal. This strategy offers the alternative with the highest historical choice probability at a 99% availability. Conversely, when $\eta \geq 0.5$, the diversified Strategy 4, which provides three non-baseline alternatives each at a 40% availability, becomes the superior choice. This transition highlights a managerial insight that when confidence in historical data is high, a concentrated strategy focused on the historically dominant option is best. As uncertainty increases, a diversified strategy that spreads availability across alternatives provides a more robust performance and yields a higher worst-case expected utility. Our framework quantifies this strategic trade-off, providing a data-driven tool for managing the choice between concentration and diversification under preference ambiguity.

4.4. Computational performance

In this section, we discuss the computational performance of the algorithm. All experiments are conducted on a MacBook Pro with an Intel Core i9 CPU and 16 GB of RAM. As we discussed in Section 3.3.2, the computational complexity of the algorithm is dominated by the subproblem solution, which scales exponentially with the number of alternatives, i.e., $O(2^K)$. Therefore, we record the running time of the algorithm to solve (3.7) for different numbers of alternatives, ranging from 4 to 10. The data used in the experiments are synthetically generated, as detailed in Appendix D. The results are illustrated in Figure 8. The figure shows that the running time of the algorithm scales exponentially with the number of alternatives. This is consistent with our theoretical analysis of computational complexity. For our main supplier selection problem with 9 alternatives, the running time is approximately 7.05 minutes.

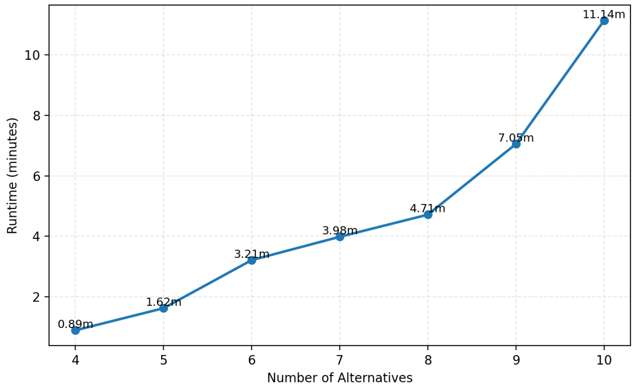

Figure 8. Computational time for solving (3.7) in a single run for different numbers of alternatives at an ambiguity radius $\eta = 0.1$, computed using synthetic data.

5. Conclusion

In this paper, we address the challenge of a single decision-maker selecting an optimal first-stage commitment strategy in a sequential planning problem. Each strategy probabilistically determines the availability of future alternatives. We develop an attribute-independent utility measure using historical choice data and use the MNL model to link utility with choice probability. To handle ambiguity in the decision-maker's own preferences, we construct an ambiguity set following the DRO approach. This enables the decision-maker to select the strategy that maximizes the worst-case expected utility, thereby making a robust choice against preference uncertainty. We show that, under reasonable conditions, the inner worst-case evaluation problem can be reformulated as a tractable convex optimization problem, which we solve using the ALM. Case studies in supply chain management and project investment demonstrate the effectiveness of our approach, highlighting its theoretical importance and practical use.

For future research, we suggest four directions: First, relaxing the exogeneity assumption on the historical choice data to incorporate potential endogeneity arising from availability constraints or strategic decisions. Second, developing more efficient computational methods to overcome the exponential complexity from summing over all possible availability subsets, especially as the number of alternatives increases. Third, enhancing the utility modeling by exploring more flexible assumptions for the random utility components. This could involve relaxing the i.i.d. assumption to account for correlations between alternatives, or investigating alternative distributional families beyond the Gumbel distribution for the error terms. Finally, extending our framework to more general ambiguity sets, such as those based on Wasserstein distance or moments. These extensions aim to improve the model's scalability, flexibility, and applicability across applications.

Author contributions

Lingyun Ji: conceptualization, methodology, software, validation, formal analysis, investigation, data curation, writing – original draft, visualization. Dali Zhang: conceptualization, methodology, resources, formal analysis, writing – review & editing, supervision, project administration. All authors have read and agreed to the published version of the manuscript.

Acknowledgments

The authors appreciate the support from National Natural Science Foundation of China with the Research Project on Human-Machine Collaborative Decision-Making (No. 72192822) and National Natural Science Foundation of China (No. 72471146).

Data availability statement

The authors confirm that the data supporting the findings of this study are available within the article.

Conflict of interest

The authors declare there is no conflict of interest.

Use of Generative-AI tools declaration

The authors declare that they did not utilize any artificial intelligence (AI) tools in the creation of this article.

References

1. L. L. Thurstone, Psychophysical analysis, *Am. J. Psychol.*, **38** (1927), 368–389. https://doi.org/10.2307/1415006
2. J. Marschak, *Binary choice constraints on random utility indications,* Stanford University Press, 1960, 312–329. https://link.springer.com/chapter/10.1007/978-94-010-9276-0-9
3. J. Simon, C. W. Kirkwood, L. R. Keller, Decision analysis with geographically varying outcomes: Preference models and illustrative applications, *Oper. Res.*, **62** (2014), 182–194. https://doi.org/10.1287/opre.2013.1217
4. F. F. Dias, P. S. Lavieri, V. M. Garikapati, S. Astroza, R. M. Pendyala, C. R. Bhat, A behavioral choice model of the use of car-sharing and ride-sourcing services, *Transp.*, **44** (2017), 1307–1323. https://doi.org/10.1007/s11116-017-9797-8
5. R. McKenna, V. Bertsch, K. Mainzer, W. Fichtner, Combining local preferences with multi-criteria decision analysis and linear optimization to develop feasible energy concepts in small communities, *Eur. J. Oper. Res.*, **268** (2018), 1092–1110. https://doi.org/10.1016/j.ejor.2018.01.036
6. F. Y. Zheng, H. Adam, P. He, Machine learning for demand estimation in long tail markets, *Manag. Sci.*, **70** (2024), 5040–5065. https://doi.org/10.1287/mnsc.2023.4893
7. Q. Feng, J. G. Shanthikumar, M. Xue, Consumer choice models and estimation: A review and extension, *Prod. Oper. Manag.*, **31** (2022), 847–867. https://doi.org/10.1111/poms.13499
8. S. Jagabathula, P. Rusmevichientong, A nonparametric joint assortment and price choice model, *Manag. Sci.*, **63** (2017), 3128–3145. https://doi.org/10.1287/mnsc.2016.2491
9. A. Aouad, V. Farias, R. Levi, Assortment optimization under consider-then-choose choice models, *Manag. Sci.*, **67** (2021), 3368–3386. https://doi.org/10.1287/mnsc.2020.3681

10. Z. H. Wang, H. Peura, W. Wiesemann, Randomized assortment optimization, *Oper. Res.*, **72** (2024), 2042–2060. https://doi.org/10.1287/opre.2022.0129

11. A. Falk, F. Zimmermann, Attention and dread: Experimental evidence on preferences for information, *Manag. Sci.*, **70** (2023), 7090–7100. https://doi.org/10.1287/mnsc.2023.4975

12. J. Forrest, A. Hafezalkotob, L. Ren, Y. Liu, P. Tallapally, Utility and optimization's dependence on decision-makers' underlying value-belief systems, *Rev. Econ. Bus. Stud.*, **14** (2021), 125–149. https://doi.org/10.47743/rebs-2021-2-0007

13. D. Ariely, K. Wertenbroch, Procrastination, deadlines, and performance: Self-control by precommitment, *Psychol. Sci.*, **13** (2002), 219–224. https://doi.org/10.1111/1467-9280.00441

14. W. B. Haskell, L. Fu, M. Dessouky, Ambiguity in risk preferences in robust stochastic optimization, *Eur. J. Oper. Res.*, **254** (2016), 214–225. https://doi.org/10.1016/j.ejor.2016.03.016

15. J. Wu, W. B. Haskell, W. Huang, H. Xu, Preference robust optimization with quasi-concave choice functions for multi-attribute prospects, *arXiv preprint, arXiv: 2008.13309*, 2020. https://doi.org/10.48550/arXiv.2008.13309

16. W. B. Haskell, H. F. Xu, W. J. Huang, Preference robust optimization for choice functions on the space of cdfs, *SIAM J. Optim.*, **32** (2022), 1446–1470. https://doi.org/10.1137/20M1316524

17. J. Hu, D. L. Zhang, H. F. Xu, S. N. Zhang, Distributional utility preference robust optimization models in multi-attribute decision making, *Math. Program.*, **212** (2025), 519–565. https://doi.org/10.1007/s10107-024-02114-y

18. J. Liu, Z. Chen, H. Xu, Multistage utility preference robust optimization, *arXiv preprint, arXiv:2109.04789,* 2021. https://doi.org/10.48550/arXiv.2109.04789

19. E. Cascetta, Random utility theory, *Transportation Systems Analysis*, Springer, USA, 2009.

20. G. Berbeglia, A. Garassino, G. Vulcano, A comparative empirical study of discrete choice models in retail operations, *Manag. Sci.*, **68** (2022), 4005–4023. https://doi.org/10.1287/mnsc.2021.4069

21. T. C. Nguyen, J. Robinson, J. A. Whitty, S. Kaneko, T. C. Nguyen, Attribute non-attendance in discrete choice experiments: A case study in a developing country, *Econ. Anal. Policy*, **47** (2015), 22–33. https://doi.org/10.1016/j.eap.2015.06.002

22. D. K. Lew, J. C. Whitehead, Attribute non-attendance as an information processing strategy in stated preference choice experiments: Origins, current practices, and future directions, *Mar. Resour. Econ.*, **35** (2020), 285–317. https://doi.org/10.1086/709440

23. S. Washington, S. Ravulaparthy, J. M. Rose, D. Hensher, R. Pendyala, Bayesian imputation of non-chosen attribute values in revealed preference surveys, *J. Adv. Transp.*, **48** (2014), 48–65. https://doi.org/10.1002/atr.201

24. Y. Y. Zhao, J. Pawlak, J. W. Polak, Inverse discrete choice modelling: Theoretical and practical considerations for imputing respondent attributes from the patterns of observed choices, *Transp. Plan. Technol.*, **41** (2018), 58–79. https://doi.org/10.1080/03081060.2018.1402745

25. A. Désir, V. Goyal, B. Jiang, T. Xie, J. W. Zhang, Robust assortment optimization under the Markov chain choice model, *Oper. Res.*, **72** (2024), 1595–1614. https://doi.org/10.1287/opre.2022.2420

26. Q. Jin, D. Z. Long, Y. Sun, B. Hu, Distributionally robust discrete choice model and assortment optimization, 2022.

27. K. Natarajan, M. Song, C. P. Teo, Persistency model and its applications in choice modeling, *Manag. Sci.*, **55** (2009), 453–469. https://doi.org/10.1287/mnsc.1080.0951
28. C. Thrane, Examining tourists' long-distance transportation mode choices using a multinomial logit regression model, *Tourism Manage. Perspect.*, **15** (2015), 115–121. https://doi.org/10.1016/j.tmp.2014.10.004
29. C. Mussida, L. Zanin, Determinants of the choice of job search channels by the unemployed using a multivariate probit model, *Soc. Indic. Res.*, **152** (2020), 369–420. https://doi.org/10.1007/s11205-020-02439-z
30. D. A. Field, Laplacian smoothing and Delaunay triangulations, *Commun. Appl. Numer. Methods*, **4** (1988), 709–712. https://doi.org/10.1002/cnm.1630040603
31. E. Delage, Y. Y. Ye, Distributionally robust optimization under moment uncertainty with application to data-driven problems, *Oper. Res.*, **58** (2010), 595–612. https://doi.org/10.1287/opre.1090.0741
32. D. McFadden, Conditional logit analysis of qualitative choice behavior, *Frontiers in Econometrics.*, Academic Press, New York, 1974, 105–142. https://escholarship.org/uc/item/61s3q2xr
33. M. Ben-Akiva, S. R. Lerman, *Discrete choice analysis*, MIT Press, USA, 1985.
34. T. P. Dence, J. B. Dence, A survey of Euler's constant, *Math. Mag.*, **82** (2009), 255–265. https://doi.org/10.4169/193009809X468689
35. M. R. Hestenes, Multiplier and gradient methods, *J. Optim. Theory Appl.*, **4** (1969), 303–320. https://doi.org/10.1007/BF00927673
36. E. G. Birgin, J. M. Martínez, Practical augmented Lagrangian methods for constrained optimization, *Society for Industrial and Applied Mathematics,* Philadelphia, USA, 2014. https://doi.org/10.1137/1.9781611973365
37. H. Y. Liu, J. Hu, Y. F. Li, Z. W. Wen, *Computational methods for optimization*, Higher Education Press, China, 2020.
38. I. Goodfellow, Y. Bengio, A. Courville, *Deep learning*, MIT Press, USA, 2016. https://doi.org/10.1007/s10710-017-9314-z
39. R. I. Boţ, E. R. Csetnek, D. K. Nguyen, Fast augmented Lagrangian method in the convex regime with convergence guarantees for the iterates, *Math. Program.*, **200** (2023), 147–197. https://doi.org/10.1007/s10107-022-01879-4

AIMS Press